

Trace Analysis of DNA: Preconcentration, Separation, and Electrochemical Detection in Microchip Electrophoresis Using Au Nanoparticles

Muhammad J. A. Shiddiky and Yoon-Bo Shim*

Department of Chemistry, Pusan National University, Keumjeong-ku, Busan 609-735, South Korea

We have developed a simple and sensitive on-chip preconcentration, separation, and electrochemical detection (ED) method for trace analysis of DNA. The microchip comprised of three parallel channels: the first two are for the field-amplified sample stacking and subsequent field-amplified sampled injection steps, while the third one is for the microchip gel electrophoresis (MGE) with ED (MGE-ED). To improve preconcentration and separation performances of the method, the stacking and separation buffers containing the hydroxypropyl cellulose (HPC) matrix were modified with gold nanoparticles (AuNPs). The formation of AuNPs and HPC/AuNP-modified buffers were characterized by UV–visible spectroscopy and TEM experiments. The conducting polymer-modified electrode was also modified with AuNPs to enhance detection performances of the electrode. The conducting polymer/AuNP layers act as electrocatalysts for the direct detection of DNA based on their oxidation in a solution phase. The total sensitivity was improved by ~25 000-fold when compared with a conventional MGE-ED analysis. The calibration plots were linear ($r^2 = 0.9993$) within the range of 0.003–1.0 pg/ μ L for a 20-bp DNA sample. The sensitivity was 0.20 nA/(fg/ μ L), with a detection limit of 5.7 amol in a 50- μ L sample, based on S/N = 3. The applicability of the method for the analysis of 13 fragments present in a 100-bp DNA ladder was successfully demonstrated.

Since highly sensitive and selective detection of DNA is of central importance to forensic, medical diagnostics, and evolutionary studies,¹ many efforts have been made to develop portable and affordable microchip devices.² Although the microchip has revolutionized biochemical and biological testing, its use in trace analysis of analytes is somewhat restricted owing to the small sample injection volume and the short path length available for optical measurements. To overcome this limitation, one promising alternative is to preconcentrate the sample prior to detection. Until now, various DNA preconcentration methods using electrokinetic trapping,^{3a} a capture device in a flowing stream,^{3b} size exclusion,^{3c} membrane-mediated loading technique,^{3d} isotachopheresis,^{3e} base stacking,^{3f} and electroosmotic flow (EOF)^{3g} have been employed in microchip and traditional capillary electrophoresis. However, the sensitivity enhancement of these methods is sometimes not

enough for trace analysis of DNA. Thus, the demand for a simple, miniature, and sensitive preconcentration method for analyzing DNA has recently arisen.

Among other preconcentration methods, field-amplified sample stacking (FASS) and field-amplified sample injection (FASI) are the most widely used in traditional and microchip electrophoresis systems.^{4–6} However, the implementation of these methods into microchip systems suffers from a major difficulty in controlling the flow and analyte movements inside the microchannel due to open communication between the various channels.^{4e} In solving the difficulty, gated injection,^{4a} a complicated channel structure,^{4b} and a porous polymer film^{4c} were previously used. Recently, an on-chip preconcentration method using a T-cross channel as an open system was demonstrated that allowed a sensitivity enhancement factor of only 160-fold.^{4e} More recently, we have developed an on-chip preconcentration technique coupled with electrochemical detection (ED) for the analysis of phenolics, which reduced the complexity in microchip structures and associated chip operations and enabled a sensitivity enhancement factor of 5200-fold.⁵ Until now, to the best of our knowledge, FAAS and subsequent FASI methods have not yet been used for DNA preconcentration in microchannels coupled with electrochemical detection.

The most commonly used detection technique adopted for DNA in preconcentration methods is laser-induced fluorescence (LIF) technique.^{3,6} Although lower detection limits can be obtained with the use of LIF, it requires derivatization of analytes. Use of electrochemical techniques instead of fluorescence can allow for simpler and smaller detectors.⁷ High sensitivity, low cost, compatibility with advanced miniaturization technologies, and direct electronic readout of detectors are the other advantages of the electrochemical techniques.^{7,8} Usually, electrochemical signals for

* Corresponding author. Phone: (+82) 51 510 2244. Fax: (+82) 51 514 2430. E-mail: ybshim@pusan.ac.kr.

- (1) (a) Park, S.-J.; Taton, T. A.; Mirkin, C. A. *Science* **2002**, *295*, 1503. (b) Drummond, T. G.; Hill, M. G.; Barton, J. K. *Nat. Biotechnol.* **2003**, *21*, 1192.
- (2) (a) Dittrich, P. S.; Tachikawa, K.; Manz, A. *Anal. Chem.* **2006**, *78*, 3887. (b) Auroux, P.-A.; Koc, Y.; deMello, A.; Manz, A.; Day, P. J. R. *Lab Chip* **2004**, *4*, 534.

- (3) (a) Dai, J.; Ito, T.; Sun, L.; Crooks, R. M. *J. Am. Chem. Soc.* **2003**, *125*, 13026. (b) Park, S.-R.; Swerdlow, H. *Anal. Chem.* **2003**, *75*, 4467. (c) Khandurina, J.; Jacobson, S. C.; Waters, L. C.; Foote, R. S.; Ramsey, J. M. *Anal. Chem.* **1999**, *71*, 1815. (d) Guttman, A. *Anal. Chem.* **1999**, *71*, 3598. (e) Wainright, A.; Nguyen, U. T.; Bjornson, T.; Boone, T. D. *Electrophoresis* **2003**, *24*, 3784. (f) Xiong, Y.; Park, S.-R.; Swerdlow, H. *Anal. Chem.* **1998**, *70*, 3605. (g) Hsieh, M.-M.; Tseng, W.-L.; Chang, H.-T. *Electrophoresis* **2000**, *21*, 2904.
- (4) (a) Jacobson, S. C.; Ramsey, J. M. *Electrophoresis* **1995**, *16*, 481. (b) Lichtenberg, J.; Verpoorte, E.; de Rooij, N. F. *Electrophoresis* **2001**, *22*, 258. (c) Jung, B.; Bharadwaj, R.; Santiago, J. G. *Electrophoresis* **2003**, *24*, 3476. (d) Beard, N. P.; Zhang, C.-X.; de Mello, A. *Electrophoresis* **2003**, *24*, 732. (e) Gong, M.; Wehmeyer, K. R.; Limbach, P. A.; Arias, F.; Heineman, W. R. *Anal. Chem.* **2006**, *78*, 3730.
- (5) Shiddiky, M. J. A.; Park, H.; Shim, Y.-B. *Anal. Chem.* **2006**, *78*, 6809.
- (6) (a) Lichtenberg, J.; de Rooij, N. F.; Verpoorte, E. *Talanta* **2002**, *56*, 233. (b) Breadmore, M. C. *Electrophoresis* **2007**, *28*, 254.

DNA are obtained either directly from the oxidation of nucleobases or indirectly using DNA-specific redox-active indicators, DNA-mediated redox-active compounds, or enzymes immobilized upon DNA hybridization.^{1b} Recently, some electrochemical methods for the direct detection of DNA have been developed based on the oxidation of the nucleobases with the conducting polymer-modified electrodes.⁸ While these methods simplify the detection scheme, their sensitivity, however, is still not enough to detect trace analysis of DNA and they are not related to preconcentration methods.

Conducting polymer has received considerable attention as the immobilizing matrix for biomolecules in biosensor systems and as catalytic layers for the detection of biomolecules including DNA hybridization.⁹ The nanoparticle comprising conducting polymer poly(5,2':5,2''-terthiophene-3'-carboxylic acid) (pTTCA) exhibited high surface areas that gave advantages to immobilize a large amount of biomolecules through covalent bond formation and, consequently, offered stable and sensitive biosensors.⁹ On the other hand, metal nanoparticles have received wide attention as electrocatalysts for electrochemical reactions that offer excellent prospects for designing highly sensitive and selective bioassays.¹⁰ The signal enhancements associated with the use of metal nanoparticles have been used in bioanalysis to increase the sensitivity of the electrochemical detectors. Of the metal nanoparticles, gold nanoparticles (AuNPs) have widely been used in bioanalysis due to size-dependent electrical property, high surface area-to-volume ratio, high electrocatalytic activity, ease of chemical modification, and structural and functional compatibility with biomolecules, particularly in DNA analysis.^{10c} Thus, AuNPs were electrodeposited onto a conducting polymer-modified electrode to enhance its electrocatalytic activity for the direct detection of DNA based on the dsDNA oxidation in a solution phase. This detection scheme eliminated the need for labeling of nanoparticles and nucleic acids. It also eliminates the use of enzymes for the amplified detection of DNA.

The utility of nanoparticles in separation sciences has attracted attention in the recent years.¹¹ The first use of colloidal AuNPs in a microchip system was demonstrated for the analysis of structural isomers of aromatic bases.^{11b} Recently, poly(ethylene oxide) (PEO) containing AuNPs and PEO adsorbed on AuNPs have also been used for the separation of DNA ranging in size from 8 to several thousand base pairs (bp) in traditional capillary electrophoresis.^{11c} In these studies, the interactions between the DNA and citrate ions, DNA and polymer/AuNP matrix, and AuNPs and channel wall were used to improve the separation performances of DNA. These interactions can also be useful for the preconcentration of DNA in microchip electrophoresis. However, to date, there is no report available to understand the impact of AuNPs on the on-chip DNA preconcentration. Thus, we tried to develop a new approach using AuNPs as both the separation and stacking buffers modifier to improve the stacking and separation performances.

The aim of this study is to develop a simple, sensitive, and direct method for analyzing DNA by integrating preconcentration steps with a separation step on a microchip with the modification of the FASS and FASI steps. The microchip consisted of two preconcentration channels to facilitate sample preconcentration by FASS and modified-FASI steps and a separation channel for

the microchip gel electrophoresis (MGE). To improve the preconcentration and separation performances, the preconcentration and separation buffers were examined with the modification of citrate-stabilized AuNPs. A pTTCA/AuNP-modified microelectrode was used to attain a sensitive and direct detection scheme for DNA. Various experimental parameters affecting the analytical performances, such as buffer concentration, water plug length, hydroxypropyl cellulose concentration in the separation buffer, AuNPs concentration, preconcentration time, detection potential, electrode-to-channel distance, and separation field strength, were assessed and optimized.

EXPERIMENTAL SECTION

Reagents. Hydroxypropyl cellulose (100 000 MW), dichloromethane (99.8%, anhydrous, sealed under N₂ gas), gold chloride trihydrate, trisodium citrate, sodium borohydride, and tris(hydroxymethyl)aminomethane were received from Sigma-Aldrich and were used as received. Tetrabutylammonium perchlorate (TBAP, electrochemical grade) was purchased from Fluka and then dried under vacuum at 10⁻⁵ Torr. A terthiophene monomer bearing a carboxylic acid group, 5,2':5,2''-terthiophene-3'-carboxylic acid was synthesized according to a previously reported procedure.¹² Sodium acetate, acetic acid, sodium hydroxide, and sulfuric acid were obtained from Aldrich. Standard DNA samples of 20-bp (5'-AAT ACC ACA TCA TCC ATA TA-3'), 42-bp (5'-ACT-GCT-AGA-GAT-TTT-CCA-CAC-TGA-CTA-AAA-GGG-TCT-GAG-GGA-3'), and a 100-bp DNA ladder (135 ng/ μ L) containing 13 dsDNA fragments ranging in sizes from 100 to 1000 bp, in 100-bp increments, and additional fragments of 1200, 1600, and 2000 bp were obtained from Bioneer Co. The 100-bp DNA ladder contains 10 mM Tris-HCl (pH 8.0), 3 mM CaCl₂, and 1 mM EDTA with some organic dyes. The stock solutions of DNA sample and standard 100-bp DNA ladder (1.0 ng/mL) were prepared in a 1.0 mM Tris-HCl buffer (pH 8.4), and subsequent dilutions were carried out daily in a 1.0 mM Tris-HCl buffer (pH 8.4). Tris-HCl buffer (100 mM, pH 8.4) was used as stacking buffer in the FASS step, and Tris-HCl (20 mM, pH 7.0) was used as detection buffer in MGE with the ED (MGE-ED) step.

Instrumentation. All electrochemical experiments were performed using a potentiostat/galvanostat, Kosentech model KST-P1. A Spellman CZE 1000R (NY) was used for supplying high voltages. AFM images were obtained with a Topometrix Discover System TMX 2010 using a commercially available Si₃N₄ cantilever with a force constant of 0.04 N m⁻¹. SEM images were obtained with a Cambridge Stereoscan 240 at KBSI. UV-visible spectra were obtained using UV-3101PC, Shimadzu. A JEOL JEM-2010

- (7) (a) Kuhr, W. G. *Nat. Biotechnol.* **2000**, *18*, 1042. (b) Willner, I. *Science* **2002**, *298*, 2407. (c) Fan, F.-R. F.; Bard, A. J. *Science* **1997**, *277*, 1791.
- (8) (a) Wang, J.; Jiang, M.; Mukherjee, B. *Anal. Chem.* **1999**, *71*, 4099. (b) Gore, M. R.; Szalai, V. A.; Ropp, P. A.; Yang, I. V.; Silverman, J. S.; Thorp, H. H. *Anal. Chem.* **2003**, *75*, 6586. (c) Shiddiky, M. J. A.; Park, D.-S.; Shim, Y.-B. *Electrophoresis* **2005**, *26*, 4656.
- (9) (a) Rahman, M. A.; Kwon, N. H.; Won, M.-S.; Choe, E. S.; Shim, Y.-B. *Anal. Chem.* **2005**, *77*, 4854. (b) Lee, T.-Y.; Shim, Y.-B. *Anal. Chem.* **2001**, *73*, 5629. (c) Ban, C.; Chung, S.; Park, D.-S.; Shim, Y.-B. *Nucleic Acids Res.* **2004**, *32*, e110/1-8.
- (10) (a) Wang, J. *Small* **2005**, *1*, 1036. (b) Daniel, M.-C.; Astruc, D. *Chem. Rev.* **2004**, *104*, 293. (c) Katz, E.; Willner, I. *Angew. Chem., Int. Ed.* **2004**, *43*, 6042.
- (11) (a) Neiman, B.; Grushka, E.; Lev, O. *Anal. Chem.* **2001**, *73*, 5220. (b) Pumera, M.; Wang, J.; Grushka, E.; Polsky, R. *Anal. Chem.* **2001**, *73*, 5625. (c) Lin, Y.-W.; Huang, M.-F.; Chang, H. T. *Electrophoresis* **2005**, *26*, 320.
- (12) Lee, T. Y.; Shim, Y.-B.; Shin, S. C. *Synth. Met.* **2002**, *126*, 105.

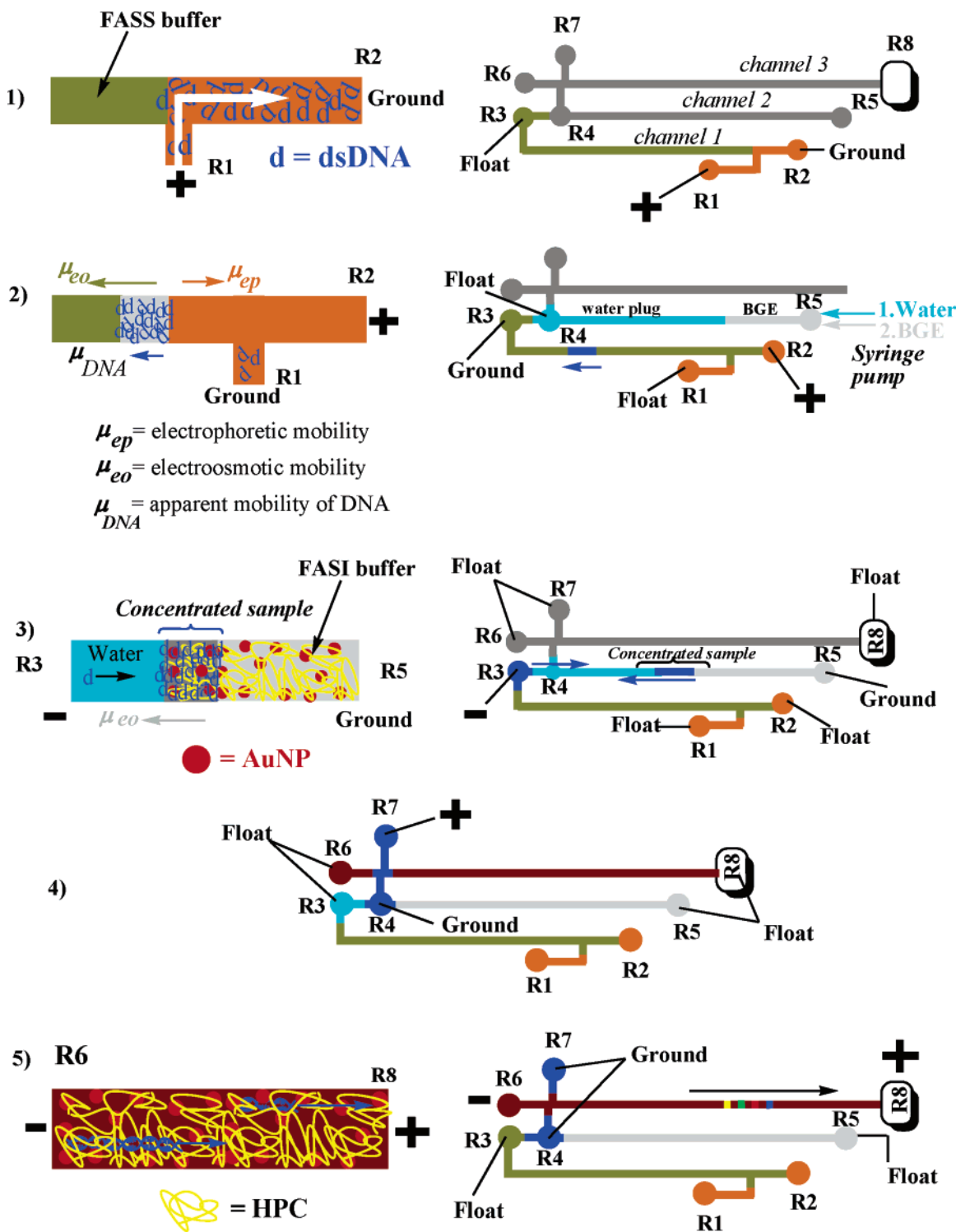


Figure 1. Schematic illustration of the preconcentration, separation, and electrochemical detection of DNA: (1) Sample loading: A voltage of +100 V/cm was applied to R1 while R2 was grounded and R3 was left floating. (2) FASS step: (i) A potential of +200 V/cm was applied to R2 for 130 s while R3 was grounded and R1 and R4 were left floating. (ii) Water/stacking buffer injection: during FASS step, a water plug was injected hydrodynamically from R5 to R4 at a flow rate of $\sim 0.1 \mu\text{L}/\text{min}$ for 110 s. Thereafter, the stacking buffer was injected for 60 s at the same flow rate. (3) FASI step: Initially preconcentrated sample was then injected into channel 2 by applying a voltage of $-150 \text{ V}/\text{cm}$ to R3 with R5 grounded, leaving all other reservoirs floating. (4) Sample loading and injection: A voltage of +100 V/cm was applied to R7 for 40 s, while R4 was grounded and R3, R5, R6, and R8 remain floating. Injection was effected by applying an injection voltage of +200 V/cm for 5 s to R4. (5) Separation and detection: MGE-ED was performed by applying a separation field strength of -340 V to R6 and $+1500 \text{ V}$ to R8 with R3, R4, R5, and R7 floating. Amperometric detection potential: $+0.8 \text{ V}$ vs Ag/AgCl.

electron microscope (Jeol High-Tech. Co.) with an acceleration voltage of 200 kV was used to obtain TEM images.

Microfabrication. Channel pattern on the microchip shown in Figure 1 was fabricated by a procedure similar to that in our

previous reports.^{5,13} The separation channel (channel 3, from R6 to R8, $l = 92 \text{ mm}$) consisted of a $150\text{-}\mu\text{m}$ double-tee injector.

(13) Shiddiky, M. J. A.; Kim, R.-E.; Shim, Y.-B. *Electrophoresis* 2005, 26, 3043.

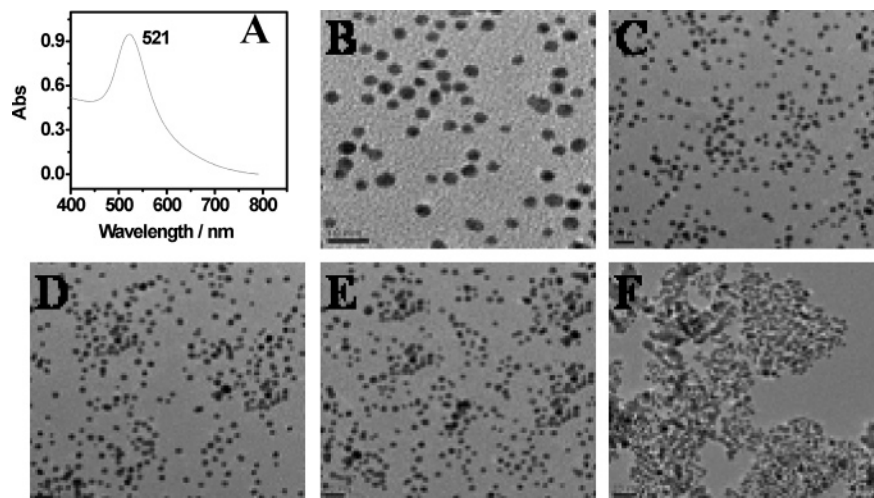


Figure 2. UV–visible (A) and TEM image (B) of AuNP solutions. TEM images of separation buffer solutions were collected (C) before and after MGE-ED run at (D) 100, (E) 200, and (F) 400 V/cm.

Channel 1 (from R2 to R3, $l = 60$ mm) included a narrow sample channel (NSC) tee injector.^{4d,14} The width of NSC is $25\ \mu\text{m}$, which is the one-sixth the width of channel 1. The distance between the injection intersection and the sample waste reservoir 1 (R2) defines the sample plug length. It allows the injection of ~ 2.0 -mm sample plug into channel 1. The length of channel 2 (from R4 to R5) was 80 mm. The depth of all channels was $\sim 23\ \mu\text{m}$. The width of the channels 1, 2, and 3 were 150, 150, and $100\ \mu\text{m}$, respectively. A homemade Teflon reservoir (i.d. 1.0 mm) was sandwiched onto each hole of the microchip using epoxy glue. The microsyringe needle was connected to the stacking buffer reservoir 2 (R5) with a custom-built Teflon screw with an O-ring through a fused-silica capillary tube (i.d. $250\ \mu\text{m}$; o.d. $350\ \mu\text{m}$) using epoxy-based glue. Platinum wire was inserted into the individual reservoir for voltage contacts.

The details of the fabrication procedure for a $100\text{-}\mu\text{m}$ Pt microelectrode was described previously.^{9a} A Teflon base was fabricated for holding the microchip and for housing the amperometric detector. The detector consisted of an Ag/AgCl reference, a Pt-wire counter, and a pTTCA/AuNP-modified working electrode and was placed in the detection reservoir (R8), where the working electrode aligned horizontally to the exit of the separation channel outlet. The distance between the channel exit and working electrode surface was controlled by a screw, which was further confirmed with a microscope (iTPRO, model 3.0).

Synthesis of Colloidal AuNPs. AuNPs were synthesized according to the previously reported procedure.¹⁵ First, a 20-mL aqueous solution containing 2.5×10^{-4} M HAuCl₄ and 2.5×10^{-4} M trisodium citrate was prepared in a conical flask. Next, 0.6 mL of ice-cold freshly prepared 0.1 M NaBH₄ solution was added to the mixture solution while stirring. Upon this addition, the solution turned pink, indicating particle formation. An adsorption band at 521 nm in the UV–visible spectrum (Figure 2A) and TEM images (Figure 2B) confirmed that the particles size in this solution was ~ 3.5 nm. The concentration of nanoparticles was calculated by following the previously described procedure^{11a} and was estimated to be to be 188 nM for ~ 3.5 -nm AuNPs. The desired dilutions were carried out daily in appropriate buffer solutions.

Modification of Stacking and Separation Buffers with AuNPs. Hydroxypropyl cellulose (HPC) was used as an adsorptive coating separation matrix because of its low viscosity, allowing the microchannel filling to be performed with ease.¹⁶ Additionally, it avoids the need for any surface modification or conditioning of the channels' surfaces and problems associated with coating inhomogeneity, channel fouling, and limited stability. To modify the stacking buffer in the FASI step, a 100 mM acetate buffer (pH 5.5) containing 20.0 nM citrate-stabilized AuNPs and 0.1 mM trisodium citrate was prepared and 2% HPC (w/v) was weighted and gradually added to the mixture solution while stirring. After the addition was complete, the suspension was stirred overnight at room temperature. Finally, it was degassed under vacuum. The separation buffer, consisting of 20 mM Tris-HCl buffer (pH 5.5), 20.0 nM citrate-stabilized AuNPs, 0.1 mM trisodium citrate, and 2% HPC, was prepared following the same method for stacking buffer in the FASI step.

Preparation of the pTTCA/AuNP Layer on a Pt Microelectrode. Before modification of the Pt microelectrode, it was cleaned by cycling the potential between 1.6 and -0.16 V several times in a 0.1 M H₂SO₄ solution at a scan rate of 100 mV/s. The electropolymerization of the conducting polymer was carried out in a 0.1 mM TBAP/CH₂Cl₂ solution by cycling the potential between 0 and 1.6 V three times at a scan rate of 1000 mV/s. After that, the electrode was washed with CH₂Cl₂ to remove the excess amount of monomer. The size of the particles of conducting polymer covered on the electrode surfaces was found to be in the range of 10–40 nm, and the thickness obtained from three cycles was estimated to be ~ 90 nm. These estimations were based on SEM and high-resolution AFM images.^{9a} AuNPs were electrodeposited on to the pTTCA-coated electrode from a 0.5 M H₂SO₄ solution containing 0.25 mM HAuCl₄ using linear sweep voltammetry from 1.5 to 0.5 V. The electrodeposition conditions were as follows: deposition time 30 s; deposition potential -0.6 V; scan rate 100 mV/s. The size of deposited AuNPs onto the conducting polymer layer was estimated in the range of 25–40 nm (based on the SEM images, not shown).

(14) Zhang, C.-X.; Manz, A. *Anal. Chem.* **2001**, *73*, 2656.

(15) Jana, N.; Gearheart, L.; Murphy, C. J. *Langmuir* **2001**, *17*, 6782.

(16) Sanders, J. C.; Breadmore, M. C.; Kwok, Y. C.; Horsman, K. M.; Landers, J. P. *Anal. Chem.* **2003**, *75*, 986.

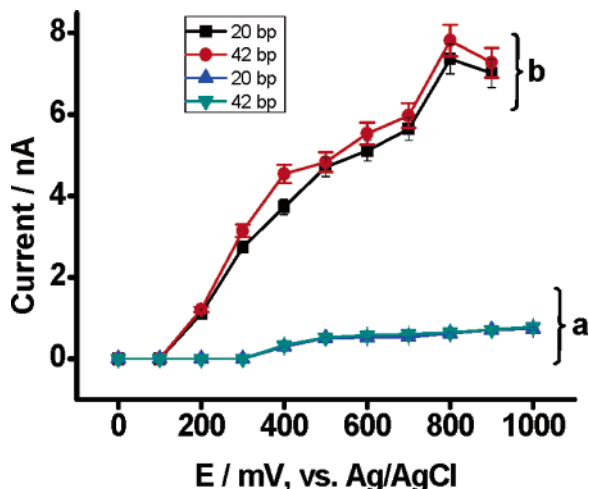


Figure 3. Hydrodynamic voltammograms for 0.05 $\mu\text{g}/\mu\text{L}$ 20- and 42-bp DNA at the (a) bare and (b) pTTCA/AuNP-modified electrodes. Separation field strength, +200 V/cm; injection time, 5 s at +200 V/cm; separation buffer, 20 mM Tris-HCl containing 2.0% HPC, 0.1 mM citrate, and 20 nM AuNPs (pH 5.5), detection buffer, 20 mM Tris-HCl (pH 7.0), and channel exit-to-electrode distance, 20 μm .

Preconcentration and the MGE-ED Procedure. After precleaning channels of the microchip,⁵ it was dried at 30 °C for 1 h. Thereafter, channel 1 was filled with the Tris-HCl buffer (100 mM, pH 8.4) by creating a vacuum to the preconcentrated sample reservoir 1 (R3). Then, the sample inlet reservoir (R1) was filled with 50 μL of the DNA sample, and the NSC tee injector was filled with the sample by applying 500 V between R1 and R2 until the current stabilized while R3 kept floating. In the FASS step, the sample was injected by applying +100 V/cm to R1 for 30 s. Subsequently, a potential of 200 V/cm was applied at R2 for 130 s to start FASS. During the FASS step, the analytes move toward the negative electrode due to the strong EOF present inside the channel.^{4d} At the boundary, the analytes decelerated and formed a narrow sample zone, giving rise to sample concentration.⁴ At the same time, a water plug was injected with a syringe pump (KDS-200, KDS Scientific) from R5 to the preconcentrated sample reservoir 2 (R4) at a flow rate of $\sim 0.1 \mu\text{L}/\text{min}$ for 110 s. Subsequently, the stacking buffer in FASI step was injected for 60 s at the same flow rate and position. Upon this step, a ~ 55 -mm length of channel 2 was filled with the low-conductivity water and the remaining (~ 28 mm) length with a high-conductivity

stacking buffer zone. Thereafter, a potential of $-150 \text{ V}/\text{cm}$ was applied to R3 for ~ 125 s (110 s for the 100-bp DNA ladder) to start FASI. Under this condition, the DNA velocity would be high in the water zone. Consequently, DNA moved toward the boundary passing through the water plug and stacked to form a concentrated sample zone at the water/buffer boundary, where the velocity of DNA dropped sharply. During this step, the water plug was moved out of channel 2 from R3 by the EOF (toward the R3 reservoir) induced by the electric field.⁵ After this step, the sample zone arrived at R4. Subsequently, the MGE-ED experiment was initiated. In this step, the separation buffer reservoir (R6) and the sample waste reservoir 2 (R7) were filled with 50 μL of separation buffer solution. The detection reservoir was filled with a 1.0 mL of detection buffer. The separation channel was filled with a separation buffer solution by applying 500 V between R6 and R8 until the current stabilized while R4 and R7 allowed floating. Sample loading was done by applying the potential of 100 V/cm to R7 for 40 s, while R4 was grounded and R6 and R8 allowed floating. The sample was injected after achieving the stable baseline by applying a potential of 200 V/cm to R4 for 5 s, while R8 was grounded and R6 and R7 allowed floating. Subsequently, the separation was carried out by applying a potential of -340 V to R6 and $+1500 \text{ V}$ to the R8 reservoir, while R4 and R7 were held at ground. This operation resulted in the field strength of 200 V/cm.

RESULTS AND DISCUSSION

Electrocatalytic Activity of the pTTCA/AuNP-Modified Electrode. To illustrate the electrocatalytic activity of the pTTCA/AuNP-modified electrode to the DNA oxidation, it was compared with the pTTCA-modified and bare electrodes in MGE-ED. Figure 4A shows the electropherograms obtained for 20-bp DNA at (a) a bare, (b) pTTCA-, and (c) pTTCA/AuNP-modified electrodes after the preconcentration and separation. For all electrodes, the peak for 20-bp DNA was visible at the migration time of ~ 87.5 s. The increased peak current and the decreased half-peak width were observed with the modified electrodes. As can be seen in Figure 4A (a), the half-peak width (~ 7.12 s) with the bare electrode was significantly larger than that obtained with the pTTCA- and pTTCA/AuNP-modified electrodes (~ 2.73 and ~ 1.94 s, respectively). At the pTTCA- and pTTCA/AuNP-modified electrodes, the peak current was increased about 4 and 10 times, respectively, as compared with a bare electrode. The separation

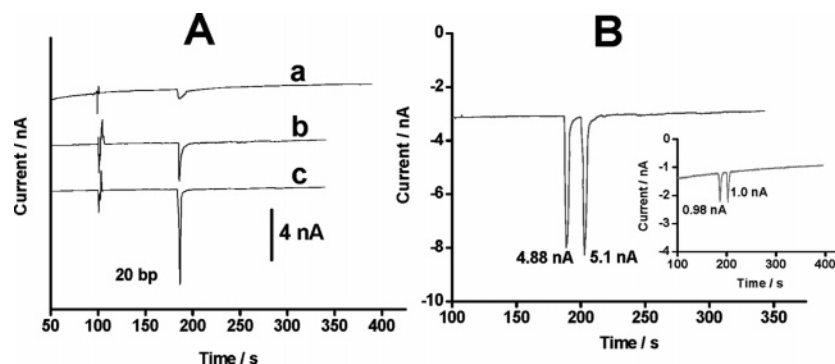


Figure 4. (A) Electropherograms of 0.05 $\mu\text{g}/\mu\text{L}$ 20-bp DNA at the (a) bare, (b) pTTCA-, and (c) pTTCA/AuNP-modified electrodes. (B) Comparison of electropherograms for 20- and 42-bp DNA samples obtained before (inset) and after (main plot) the FASS and subsequent FASI steps in MGE-ED with the pTTCA/AuNP-modified electrode. The concentration of 20- and 42-bp DNA in the inset figure was 0.1 $\text{ng}/\mu\text{L}$, whereas it was 0.02 $\text{pg}/\mu\text{L}$ each in the main plot. Detection potential was +0.8 V vs Ag/AgCl. Other experimental conditions were as in Figure 3.

efficiency (N)⁵ at the pTTCA/AuNP-modified electrode was found to be $\sim 12\,530$, whereas ~ 840 was calculated for the bare electrode. The increased peak currents with sharper peak width at the pTTCA/AuNP-modified electrodes reflect its faster electron transfer in the catalytic oxidation process of DNA. To understand the electrocatalytic activity of the modified electrode, we have performed the cyclic voltammetric experiments using the $[\text{Fe}(\text{CN})_6]^{3-/4-}$ redox system. A well-defined reversible voltammogram characteristic of a diffusion-controlled redox process was observed at the bare electrode. A significant decrease in the peak separation ($\Delta E = 118$ to 70 mV) and an increase in the peak current (~ 4 times) have been observed at the pTTCA-modified electrode. A further increase in the peak current (~ 10 times) along with a decrease in ΔE (118 to 60 mV) has been observed at the pTTCA/AuNP-modified electrode. The standard electron-transfer rate constant (k_s) was estimated using the Nicholson theory.¹⁷ The modification of the electrode surface by polymer and further by AuNPs increases the k_s value by a factor of ~ 7 and ~ 50 ($k_s^{\text{bare}} = 3.61 \times 10^{-3} \text{ cm s}^{-1}$; $k_s^{\text{pTTCA}} = 24.7 \times 10^{-3} \text{ cm s}^{-1}$, and $k_s^{\text{pTTCA/AuNPs}} = 193 \times 10^{-3} \text{ cm s}^{-1}$), respectively. We believe that the AuNP modification of the electrode surface can increase the active area of the polymer layer by increasing the contacts between polymer and AuNPs that can enhance the conductivity of the modified electrode.¹⁸ The enhanced conductivity of the pTTCA layer by the AuNP modification might have been attributed to the faster electron transfer for dsDNA oxidation.

The hydrodynamic voltammograms shown in Figure 3 also illustrated the electrocatalytic activity of the pTTCA/AuNP-modified electrode. The setup potential for the pTTCA/AuNP-modified electrode was $+200$ mV, whereas it was $+400$ mV for the bare electrode. These profiles indicate that the pTTCA/AuNP-modified electrode offers improved performances with a higher sensitivity and lower detection potential. An increase in the baseline current, its slope, and the noise levels were observed at a potential higher than 0.8 V using the pTTCA/AuNP-modified electrode. The high background current leads to an unstable baseline, which is disadvantageous in achieving a high sensitive and stable detection.^{11b} Thus, the detection potential of 0.8 V was employed for all experiments.

Preconcentration of DNA. To find out the sensitivity enhancement factor of the present method, it was compared to a conventional MGE-ED analysis. The conventional MGE-ED analysis was carried out using only channel 3 of the microchip without performing the preconcentration steps with the pTTCA/AuNP-modified electrode. Figure 4B (inset) shows a typical electropherogram obtained under this condition. The migration time, half-peak widths, and N values were ~ 87.5 and ~ 102.6 s, 1.93 and 2.63 s, and $12\,500$ and 8600 for 20- and 42-bp samples, respectively. We then performed microchip separation and electrochemical detection after the preconcentration steps for the sample mixture diluted by a factor of 5×10^3 . The result is shown in Figure 4B. The DNA samples were detected with the same migration times, half-peak widths, and separation efficiency as shown in Figure 4B (inset). It is clearly seen that the peak heights in the main figure are ~ 5 times higher than those in the inset figure. The sensitivity enhancement of the method was then evaluated by

comparing the slopes of the linear ranges for the systems before and after applying FASS and FASI steps. The slope was $8.1 \text{ nA}/(\text{ng}/\mu\text{L})$ for the system before applying preconcentration steps (linear range: $40 \text{ pg}/\mu\text{L}$ – $2 \text{ ng}/\mu\text{L}$); whereas it was $0.201 \text{ nA}/(\text{fg}/\mu\text{L})$ (linear range: 0.003 – $1.0 \text{ pg}/\mu\text{L}$) for the system after applying preconcentration steps. Comparing the two slopes, the total sensitivity enhancement was found to be $\sim 24\,900$ -fold. The reason for getting such sensitivity enhancement was due to AuNP modification of stacking/separation buffers and electrode surfaces. In the FASS step, DNA stacking occurs at the boundary between the low- and high-conductivity buffers due to the sharp decreases in the velocity of DNA migrating from the higher field strength (in low-conductivity sample buffer) to a relatively lower (in high-conductivity stacking buffer) zone.⁴ In the FASI step, stacking occurs in low-pH/high-conductivity stacking buffer containing HPC/AuNPs matrix. DNAs were stacked first at the boundary between the water and low-pH/high-conductivity buffer that was possibly for the same reason as mentioned above for the FASS step. The initially stacked DNA samples were subjected to the second stacking on the interaction with the HPC/AuNP matrix present at the concentration boundary. The second stacking occurs mainly because of retardation of DNA movement by the HPC/AuNP matrix. Additionally, the presence of trisodium citrate ions and citrate-stabilized AuNPs in the stacking buffer solution might have affected the enhancement of the stacking efficiency due to three possibilities. These include either the increasing of relative conductivity of the stacking buffer, the adsorption of DNA onto HPC/AuNP surfaces through the protruding part of the HPC matrix that adsorbed on the AuNP surfaces, and minimization of the DNA adsorption on the wall of the channel in the presence of AuNPs that are strongly adsorbed on it.^{11c} The sensitivity enhancement factor of $\sim 24\,900$ -fold is ~ 2 – 3 orders higher than those obtained by other DNA preconcentration methods.³

Optimization of Preconcentration Conditions. In initial experiments, a 20 mM Tris-HCl buffer ($\text{pH } 5.5$) was used as a separation buffer for the separation of 20- and 42-bp DNA using channel 3 of the microchip. A broadened and destroyed peak was observed (not shown), which indicated that only 20 mM Tris-HCl buffer was not enough for the separation of DNA samples. The adsorption of DNA on to the channel wall might have been responsible for such a destroyed peak. To effectively separate DNA samples by eliminating their adsorption, a buffer solution containing HPC was used. As shown in Figure 5A (b), both peaks were well separated when 20 mM Tris-HCl with 2.0% HPC was used as a separation buffer solution. The migration times for 20- and 42-bp DNA were $\sim 114 \pm 0.6$ and 145 ± 0.5 s, respectively. However, the concentration of HPC in the separation buffer has affected the separation performances of the method. The resolution between the peaks and the migration time for both analytes increase as the concentration of HPC increases (Figure 5A). The longer migration time caused by the higher HPC concentration was mainly due to the retardation effect of the HPC matrix.¹⁶ While 3.0% HPC makes for a better choice in terms of resolution, this condition, however, was not selected because of the longer migration time. The reproducibilities of the migration time and peak current were <2.8 and 4.2% ($n = 4$), respectively. These results could be due to hydrogen bonding between HPC and the

(17) Nicholson, R. S. *Anal. Chem.* **1965**, *37*, 1351.

(18) Cho, S. H.; Park, S.-M. *J. Phys. Chem. B* **2006**, *110*, 25656.

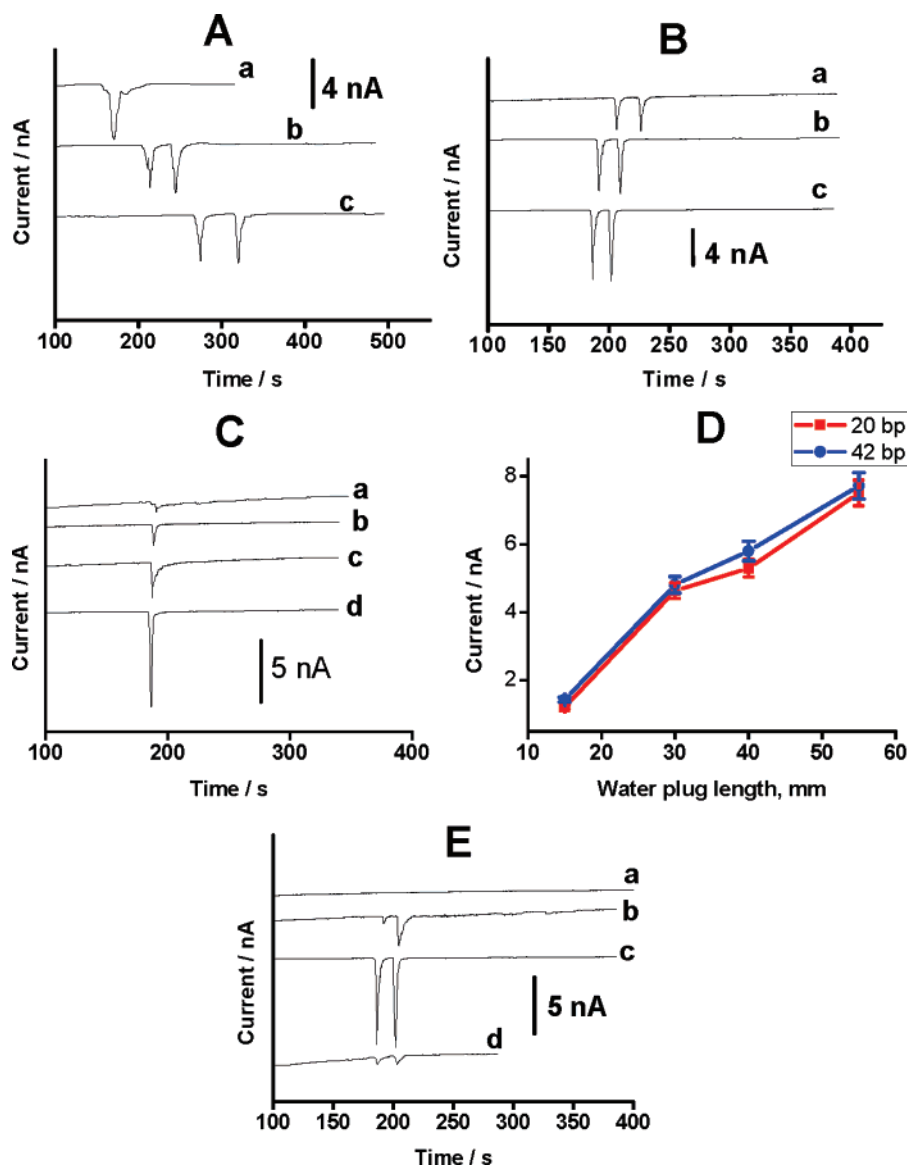


Figure 5. Effects of the (A) HPC- and (B) HPC/AuNP-modified separation buffer, (C) conductivity ratio of the stacking buffer to the sample buffer in the FASS step, (D) the water plug length, and (E) the sample preconcentration time in the FASI step for the analysis of 0.05 pg/ μ L 20- and 42-bp DNA. For (A), the separation buffer was 20 mM Tris-HCl (pH 5.5) with (a) 1.0, (b) 2.0, and (c) 3.0% HPC. For (B), the separation buffer was 20 mM Tris-HCl (pH 5.5) with the 2.0% HPC containing (a) 1.0, (b) 10, and (c) 20 nM AuNPs. For (C), sample buffers were a (a) 100, (b) 60, (c) 30, and (d) 1.0 mM Tris-HCl (pH 8.4), whereas stacking buffer was 100 mM Tris-HCl (pH 8.4). For (E), the sample preconcentration times was (a) \sim 116, (b) \sim 120, (c) \sim 125, and (d) \sim 128 s. Other experimental conditions were as in Figure 4.

channel wall¹⁶ that resulted in stable EOF and reproducible channel surfaces.

To investigate the effect of AuNPs on separation performances of the method, separation buffers containing different concentrations of AuNPs were examined (Figure 5B). The resolution between the peaks and migration times for 20 and 42 bp gradually decreased as the AuNP concentration increased from 1.0 to 20 nM. At 20 nM concentration, the migration times for 20- and 42-bp samples were \sim 87.5 and 102.6 s, respectively, which were much lower than those obtained in Figure 5A (b). The half-peak width decreased from \sim 5.49 and 5.82 to \sim 1.93 and 2.63 s giving increased N values from \sim 2300 to 12500 and \sim 3440 to 8600, for 20- and 42-bp samples, respectively. These results were possibly due to altering the EOF of the buffer and apparent mobility of

DNA by the following:¹⁹ (i) the interaction between the citrate ions (triprotic acid) and DNA molecules and (ii) the changes in the morphology of the buffer containing HPC/AuNPs due to the aggregation of the AuNPs during electrophoretic separation. These possibilities can be correlated or independent of each other. As can be seen in Figure 5B, the peak currents gradually increase upon increasing the AuNPs concentration in the separation buffer. This might have been due to increased conductivity of the sensor surface with increasing quantity of AuNPs in the separation buffer. A concentration of AuNPs higher than 20 nM resulted in poor reproducibility of the migration time ($>4.8\%$, $n = 5$) and peak current (>8.55 ; $n = 5$). Such results might have been due to the larger aggregation of the AuNPs at higher AuNP concentrations,^{11a}

(19) Huang, M.-F.; Huang, C.-C.; Chang, H.-T. *Electrophoresis* **2003**, *24*, 2896.

resulting in an unstable separation buffer solution that was supported by the TEM image (not shown).

The effect of the AuNP concentration on the sensitivity enhancement of the method was investigated by adding AuNPs in to the stacking buffer from 1.0 to 20 nM (not shown). Two peaks at ~ 87.4 and 102.7 s were detected with increased peak currents upon increasing the AuNPs concentration for 20- and 42-bp samples, respectively. The results indicated that the presence of AuNPs in stacking buffer could enhance the sensitivity factor of the method, which was possibly due to the increased interaction of DNA on HPC/AuNPs surfaces through the protruding part of HPC upon increasing AuNP concentrations. The increased conductivity of the stacking buffer in the FASI step and minimization of the samples' adsorption on to the channel wall in the presence of AuNPs might have contributed to such an occurrence. An AuNP concentration higher than 20 nM resulted in a small increase in the peak currents, which indicates that 20 nM AuNPs is sufficient to provide enough nanoparticles to enable maximum available interactions with DNAs and optimal conductivity ratio of the stacking buffer to water zone. Thus, 20 nM AuNP concentration was used for all subsequent experiments.

To examine the aggregation of nanoparticles upon separation field strengths, TEM images for separation buffer solutions were recorded. The solutions were collected from the outlet of channel 3 by applying pressure via R6 after MGE-ED runs at different separation field strengths. Figure 2C–E shows TEM images for the solutions collected after MGE-ED runs at 100, 200, and 400 V/cm, respectively. As shown in Figure 2B and C, there was very little change in particle distribution, which indicates almost no aggregation of AuNPs, occurring at lower field strengths. However, the aggregation of AuNPs gradually increased as the separation field strength was increased from 100 to 375 V/cm (Figure 2C–E). The polymer adsorbed on the AuNPs is stiffer and less extended²⁰ and, consequently, becomes deformed under the electrophoretic separation.¹⁹ The aggregation of AuNPs, which results in enhance interaction among HPC molecules, and deformation of AuNPs/HPC under the applied field strength might have been attributed to such agglomeration of separation matrix. This aggregation or agglomeration of separation matrix results in poor reproducibility of the migration time and the peak current (RSD, 12.2 and 17.6%, respectively, for $n = 3$).

The effect of the conductivity ratio of the stacking buffer to the sample buffer solution in the FASS step was investigated. When the conductivity ratio was 1, no evidence of the preconcentration was observed using only the FASS step (not shown). It was due to the equal conductivity of the sample and stacking buffer solutions.^{4e} However, when both FASS and subsequent FASI steps were involved in the preconcentration process, the peak current at the pTTCA/AuNP-modified electrode increased as the conductivity ratio increased (Figure 5C). At the ratio of 1 (a), the preconcentration occurs mainly due to the involvement of the FASI step with the FASS step. Using the conductivity ratio of 100 (d), the maximum signal enhancement was observed. However, increases of the stacking buffer concentration above 100 mM resulted in a decrease of peak currents, mainly due to Joule heating that is apparently dominant at the high buffer concentration.^{4d} Thus, 100 and 1.0 mM Tris-HCl (pH 8.4) buffers

were used as stacking and sample buffers, respectively, in the FASS step.

We have also examined the effect of direct injection of the concentrated sample to channel 3 on the sensitivity of the method by applying only the FASS step. The total sensitivity enhancement was increased by ~ 450 -fold when it was compared with a conventional MGE-ED analysis (not shown). To check the loss and dilution of the initially concentrated sample during transition from channels 1 to 3 on the sensitivity of the method, a control experiment was performed. A potential of 200 V/cm was applied to R2 in channel 1 for 130 s, while R4 instead of R3 in channel 2 was grounded for the sample preconcentration by FASS. Afterward, subsequent FASI and MGE-ED steps were started. The peak currents for 50 pg/ μ L 20- and 42-bp DNA samples were decreased by 3.5% in magnitude with the similar peak widths (RSD, 5.4%), indicating that the loss and dilution of the concentrated sample transition from channel 1 to channel 2 is not significant.

The water plug length affects the sensitivity enhancement factor and the required time in the FASI step.⁵ The water plug length was optimized by varying the length from ~ 15 to 55 mm. Figure 5D shows the effect of water plug length on the peak current of 20- and 42-bp DNA with the pTTCA/AuNP-modified electrode. The peak current increased as the plug length increased from ~ 15 to 55 mm. When the water plug length was ~ 55 mm, the sensitivity of the modified electrode was maximal, and consequently, the highest sensitivity enhancement was observed. Therefore, a water plug of ~ 55 mm was used as the optimized length.

Figure 5E shows the electropherograms obtained for different preconcentration times in the FASI step. The peaks for the 20- and 42-bp samples with the maximum peak currents were detected at the preconcentration time of ~ 125 s. However, no peaks were detected at ~ 116 s, indicating that a period of 116 s was not sufficient to bring the sample plug to R4, whereas a period of ~ 128 s could pump out the sample plug from the R4. The higher peak current for 42 bp was observed at ~ 120 s (b). This could possibly be due to the slightly higher mobility of the 20 bp than that of 42 bp in moving toward R5 because the smaller DNA fragment was retarded less effectively by the HPC matrix, and consequently, it would be placed at the rear of the stacked-sample zone. Thus, it took a slight longer time to arrive at R4. Because of this fact, when we analyzed the 100-bp DNA ladder with the preconcentration time of ~ 125 s, only the shorter DNA fragments present in the ladder were detected in lower peak currents (not shown). The longer fragments were not detected, possibly due to the pump out of these fragments from the R4 at ~ 125 s time. However, all fragments present in the DNA ladder were detected with the best sensitivity at the time of ~ 110 s. When the time was ~ 114 or ~ 106 s, some peaks in lower peak currents were observed. Thus, ~ 125 s was chosen as the preconcentration time in the FASI step for the analysis of smaller DNA fragments (20 and 42 bp), whereas ~ 110 s was chosen for the 100-bp DNA ladder analysis.

Optimization of MGE-ED Conditions. The effect of the separation field strength on the migration time, peak currents and N values in DNA analysis was investigated (not shown). The migration time decreased, while the N value increased upon increasing the field strength from 125 to 200 V/cm. Further

(20) Nowicki, W. *Macromolecules* **2002**, *35*, 1424.

increases in the field strength resulted in a decrease in separation efficiency due to the end-channel broadening and incomplete isolation of the detection system and Joule heating.^{11b,21} At the separation field strength of >300 V/cm, a poor reproducibility in migration times and peak currents and an unstable baseline were observed. The best sensitivity with the best separation efficiency, and resolution was observed at 200 V/cm. Thus, the separation field strength of 200 V/cm was used for all separations.

The distance between the channel outlet and the working electrode surface affects the peak currents and shapes of analytes at the modified electrode.^{5,8c,21} When the working electrode to channel distance increased from 20 to 200 μm , a gradual decrease of the peak current and increases of the half-peak width were observed. At a wider spacing, ED revealed an unstable baseline with high background noises. However, at a very small spacing (<20 μm), increasing levels of background noise were observed. Thus, in order to get the best sensitivity of the modified electrode, it was placed at a distance of 20 μm from the separation channel exit.

Analytical Performances. Under the optimized conditions, the reproducibility, linear dynamic range, and detection limit of the method were calculated with the pTTCA/AuNP-modified electrode. The run-to-run reproducibility was 0.8, and 1.5% for migration times and peak currents, respectively. Although the migration time and peak current varied slightly from run to run, the reproducibility of the analysis was excellent. The reproducibility in the peak current and the migration time by the modified electrode were found to be <5.2 and <2.9%, respectively, for six repetitive injections. The large variation in migration time was due to the following: (i) the changes in the concentration of separation buffer^{5,21} and (ii) the contamination of the electrode surface caused by repetitive sample injections.¹³ The stability of the pTTCA/AuNP-modified electrode was examined using 30 repetitive injections of 0.1 ng/ μL 42-bp DNA sample with an AuNP-modified electrode using only channel 3 of the microchip. A 14% decrease in the initial peak current, RSD, 11.2% for $n = 30$, was observed. The decrease of the peak current might be due to the deactivation of the electrode surfaces caused by multiple uses of the electrode. The deactivation might be attributed to the following: (i) the contamination of the electrode surface by the oxidation products or (ii) dissolution of the films with time.

A 20-bp DNA sample was used to evaluate the hydrodynamic range of the method. A broad dynamic linear range of 4 orders of magnitude from 0.003 to 1.0 pg/ μL was achieved. This is 2 orders wider of the range than that of the other on-chip preconcentration method.^{4e} The calibration plot for the 20-bp DNA sample was found to be linear with the correlation coefficient of 0.9993 over the concentration range tested, when the 42-bp DNA sample was kept constant at 0.02 pg/ μL to serve as the internal standard. The peak current for 42 bp was detected with a good reproducibility in migration times (<2.7%) and peak currents (<5.6%) ($n = 6$). The sensitivity of the method was 0.201 nA/(fg/ μL) with a detection limit of 0.7 fg/ μL , based on $S/N = 3$ (95% confidence level, $k = 3$, $n = 6$). The detection limit corresponds to 35 fg (5.67 amol) in 50 μL of 20-bp DNA sample, which is much lower than those obtained by the other DNA preconcentration methods.³ Additionally, the detection limit is ~ 1000 -fold lower than the values

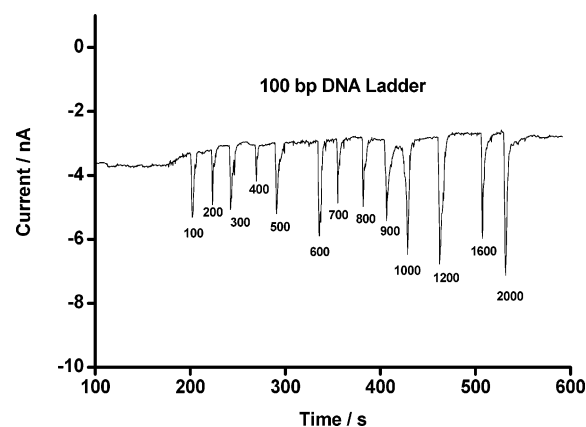


Figure 6. Electropherograms showing separations of 13 fragments present in a 100-bp DNA ladder with the pTTCA/AuNP-modified electrode. The concentration of 100, 200, 300, 400, 600, 700, 800, 900, 1200, and 1600 bp was ~ 0.01 pg/ μL ; while that for 500, 1000, and 2000 bp was ~ 0.03 pg/ μL . Other experimental conditions were as in Figure 4.

obtained using conventional DNA analysis methods with nanoparticles and cationic polythiophene-modified electrodes.²² However, this detection limit is comparable to the lowest values in recently reported electrochemical methods that employed carbon nanotube-derived amplification, multiple enzyme layers on carbon nanotube, quantum dot, DNA hybridization using biometallization, and array-based electrochemical detection of DNA.^{23,24} These methods are conceptually different from ours, because they used only the electrochemical detection without preconcentration and separation.

Application to 100-bp DNA Ladder. To evaluate the advantages of this new method, a 100-bp DNA ladder containing 13 fragments was analyzed. Figure 6 represents a typical electropherogram of a 100-bp DNA ladder obtained after the on-chip preconcentration in MGE-ED. All fragments present in the ladder were well separated and detected within ~ 435 s. The reproducibilities of the migration time and the peak current were <3.2 and <5.8% ($n = 6$), respectively. The resolution between the neighboring fragments were in the range of ~ 3.5 for 600/700 to ~ 1.35 for 900/1000 bp's. Compared with an electropherogram obtained by a conventional MGE-ED analysis (not shown), the sensitivity enhancement factor was estimated to be in the range of $\sim 23\,000$ for 400 bp to $\sim 25\,500$ folds for 2000 bp.

CONCLUSIONS

We have developed a simple and sensitive DNA analysis method by integrating the FASS and modified-FASI preconcentration steps with the MGE-ED on a microchip. The coupling of the pTTCA/AuNP-modified microelectrode with the AuNPs' modification of both the separation and stacking buffer solutions

- (22) (a) Wang, J.; Liu, G.; Merkoci, A. *J. Am. Chem. Soc.* **2003**, *125*, 3214. (b) Polsky, R.; Gill, R.; Kaganovsky, L.; Willner, I. *Anal. Chem.* **2006**, *78*, 2268–2271.
- (23) (a) Patolsky, F.; Lichtenstein, A.; Willner, I. *Angew. Chem., Int. Ed.* **2000**, *39*, 940. (b) Patolsky, F.; Lichtenstein, A.; Willner, I. *Nat. Biotechnol.* **2001**, *19*, 253. (c) Hansen, J. A.; Mukhopadhyay, R.; Hansen, J. Ø.; Gothelf, K. V. *J. Am. Chem. Soc.* **2006**, *128*, 3860.
- (24) (a) Wang, J.; Liu, G.; Jan, M. R. A. *J. Am. Chem. Soc.* **2004**, *126*, 3010. (b) Munge, B.; Liu, G.; Collins, G.; Wang, J. *Anal. Chem.* **2005**, *78*, 4662. (c) Hwang, S.; Kim, E.; Kwak, J. *Anal. Chem.* **2005**, *77*, 579.

(21) Shiddiky, M. J. A.; Won, M.-S.; Shim, Y.-B. *Electrophoresis* **2006**, *27*, 4545.

in MGE-ED was shown to be a sensitive electrochemical method for DNA analysis. The modified microelectrode displayed an improved sensitivity and reproducibility compared to a bare electrode, reflecting its electrocatalytic activity and resistance to surface fouling. The stacking and separation performance of the method was enhanced by the modification of the stacking and separation buffers with the citrate-stabilized AuNPs. The sensitivity enhancement of the present method is eventually much higher than those obtained by the other DNA preconcentration methods. Although, we obtained attomole sensitivity, it could be further improved by implementing serial preconcentration/injection channels onto a single microchip and optimizing the injection and stacking conditions. The sensitivity, efficiency, selectivity, reproducibility, miniaturization, and decreased reagent consumption in the present work suggests the possibility to perform field analysis

and diagnosis of diseases by detecting the trace level disease markers at the early stage of diseases. Unlike enzyme-based amplification scheme of DNA, the elimination of enzyme, nucleic acid, and nanoparticle labeling and the use of pTTCA/AuNPs as electrocatalyst for the direct electrochemical detection of DNA in a solution phase are other advantages for the present method.

ACKNOWLEDGMENT

This work was supported by the Ministry of Health and Welfare (A020605 and A050426), Republic of Korea and SRC program of KOSEF.

Received for review January 20, 2007. Accepted March 17, 2007.

AC0701177